Journal of Inclusion Phenomena and Molecular Recognition in Chemistry **17:** 351–363, 1994.

Spectroscopic Characterization and Electrocatalytical Activity of Tetrapyridylporphyrins Intercalated into Hydrated Vanadium(V) Oxide

HENRIQUE E. TOMA* and HERENILTON P. OLIVEIRA
Instituto de Química, Universidade de São Paulo, Caixa Postal 20780, CEP 01498–970, São Paulo, SP, Brazil.

and

HERCÍLIO R. RECHENBERG
Instituto de Física, Universidade de São Paulo, Caixa Postal 20780, CEP 01498–970, São Paulo, SP, Brazil.

(Received: 17 December 1993; in final form: 3 May 1994)

Abstract. The intercalation of *meso*-tetrapyridylporphyrins into hydrated vanadium(V) pentoxide has been studied using X-ray diffraction; FTIR, electronic and Mössbauer spectroscopy; cyclic voltammetry and spectroelectrochemistry. The intercalation compound containing iron tetrapyridylporphyrin exhibits pronounced electrocatalytical activity in the reduction of molecular dioxygen, reflecting an enhanced reactivity of the catalyst in a confined medium.

Key words: Porphyrin intercalation compounds, vanadium pentoxide films, spectroelectrochemistry, oxygen reduction, Mössbauer spectra, electrocatalysis.

1. Introduction

Vanadium pentoxide films have been extensively investigated in regard to their conducting and electrochromic properties [1–16]. The hydrated oxide can be generated by a number of procedures, exhibiting a bidimensional structure with an interlamellar distance of 1.155 nm [17, 18] suitable for the intercalation of many inorganic, organic and polymeric species [19–32]. In this work we report the synthesis, characterization and electrochemical properties of new intercalation compounds obtained by the inclusion of *meso*-tetrapyridylporphyrins into vanadium oxide xerogels. These guest molecules exhibit a planar porphyrin ring with four pyridine groups in the *meso* position, as illustrated in Figure 1, and are of great interest from the point of view of their catalytical properties in a confined medium.

---

* Author for correspondence.

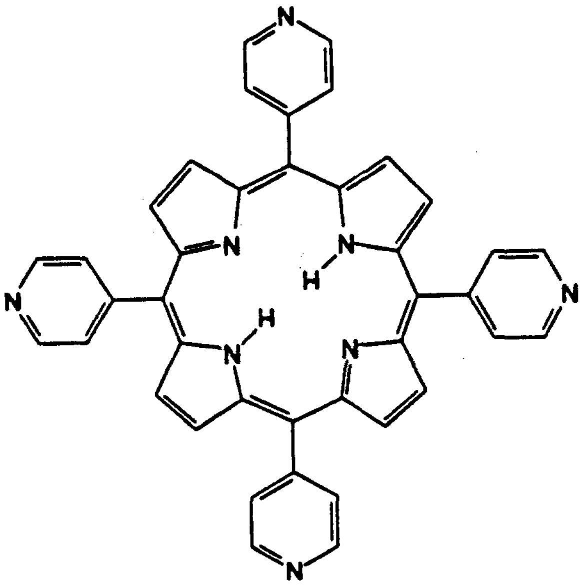

Fig. 1. *meso*-tetrapyridylporphyrin.

2. Experimental

Polyvanadic acid was prepared by ion exchange of sodium metavanadate (Alfa Ventron) as reported in the literature [33, 34]. The films were obtained by the slow evaporation of the polyvanadic acid gel on a glass plate at room temperature. The composition, based on X-ray fluorescence and thermal analysis, was consistent wiht $V_2O_5 \cdot xH_2O$, where $x = 1.9 - 2.5$. *Meso*-tetra(4-pyridyl)porphyrin (TPyP) and *meso*-tetra(4-pyridyl)porphyrin iron(III) chloride, [FeTPyP]Cl, were kindly supplied by Professor K. Araki. The intercalation compounds were obtained by treating the vanadium pentoxide films (35 mg) with small portions of a 3 mL solution containing 10 mg of the porphyrin dissolved into 0.01 M HCl, and allowing the solvent to evaporate, in a repetitive way. After a week, the films were washed with nanopure water and with acetone. The solids were dried at 60°C, exhibiting a metallic, dark blue color. The samples employed in this work gave the following analysis: $(V_2O_5)_1(TPyP)_{0.075}(H_2O)_{0.38}$, C, 14.5; N, 3.53; H, 1.59, V_2O_5, 77.4%; *calcd.* C/N, 5.0, *found*, C/N, 4.9. $(V_2O_5)_1(FeTPyP)_{0.025}(H_2O)_{0.48}$, C, 4.94; N, 1.17, H, 1.75, Fe, 1.50, V_2O_5, 86.6%, *calcd.* C/N, 5.0, *found*, C/N, 5.0.

Cyclic voltammetry was carried out using a Princeton Applied Research model 173 potentiostat, and a model 175 universal programmer. The conventional three electrode arrangement was used, consisting of a glassy carbon or a platinum disc working electrode, a platinum wire auxiliary electrode and a reference electrode of $Ag/AgNO_3$ (0.010 M) in acetonitrile or of Ag/AgCl (1.00 M KCl) in aqueous solution. Ring-disc voltammograms were obtained using a Pine/Eg&G model 366 bipotentiostat and a model 636 rotating electrode accessory. Spectro-electrochemical measurements were performed using the potentiostat attached to a Guided Wave, model 260 fiber optics instrument, or a Hewlett-Packard model 8452-A diode-array spectrophotometer. FT-IR spectra were recorded on a Bohmem, model DA3 instrument equiped with a reflectance accessory. X-ray diffraction data were recorded on a Philips, model PW 1370 instrument, or on a Rigaku-Geigerflex instrument, using Cu$K_{\alpha 1}$ emission lines (0.154 nm). Mössbauer spectra were recorded on a Wissel instrument, at room temperature, using a ^{57}Co(Rh) source, and metallic iron for calibration.

3. Results and Discussion

3.1. X-RAY DIFFRACTION

Typical X-ray diffraction patterns for the vanadium pentoxide matrix, and of the intercalation compounds with TPyP and FeTPyP are shown in Figure 2. The diffraction patterns are consistent with a lamelar structure, where the interplanar distance in the V_2O_5 matrix and in the TPyP and FeTPyP intercalation compounds are 1.18 ± 0.02, 1.26 ± 0.02 and 1.40 ± 0.03 nm, respectively. These values are smaller than the molecular radii of the TPyP and FeTPyP species, which can be estimated as 1.6 nm based on the crystallographic distances of related porphyrins. Therefore, the intercalation of the porphyrins should occur with the molecular plane nearly parallel to the V_2O_5 planes. Presumably, the porphyrins are replacing the water molecules in the interlamellar space, leading to small changes in the interplanar distances.

In the attempt to estimate the thickness (D) and the disorder factor (K') of the films, we have employed the modified Scherrer equation [35],

$$\beta \cos \theta/\lambda = 1/D + K' \sin \theta/\lambda$$

where β is the half bandwidth, θ is the diffraction angle and λ is the X-ray wavelength. The calculated values of D and K' for the vanadium pentoxide matrix and for the TPyP and FeTPyP intercalation compounds were 9.5 nm, 0.03; 7.3 nm, 0.03; and 10 nm, 0.13, respectively. Therefore, the crystallinity decreases in the following order: V_2O_5 matrix = V_2O_5–TPyP > V_2O_5–FeTPyP. The crystallinity is not exclusively related to the amount of the porphyrin in the matrix, since the diffractogram of the sample containing 19.6% TPyP (Figure 2.B) is much more defined than that of the sample containing 7.8% FeTPyP (Figure 2.C).

3.2. FTIR SPECTRA

The FTIR spectra of the intercalation compounds, in the range of 2000–800 cm^{-1}, are shown in Figure 3. In this range, the vanadium pentoxide matrix exhibits a very weak band at 1650 cm^{-1} ascribed to the δ(OH) vibrational modes of the water molecules, and two broad bands at 1005 and 760 cm^{-1} ascribed to ν(VO)

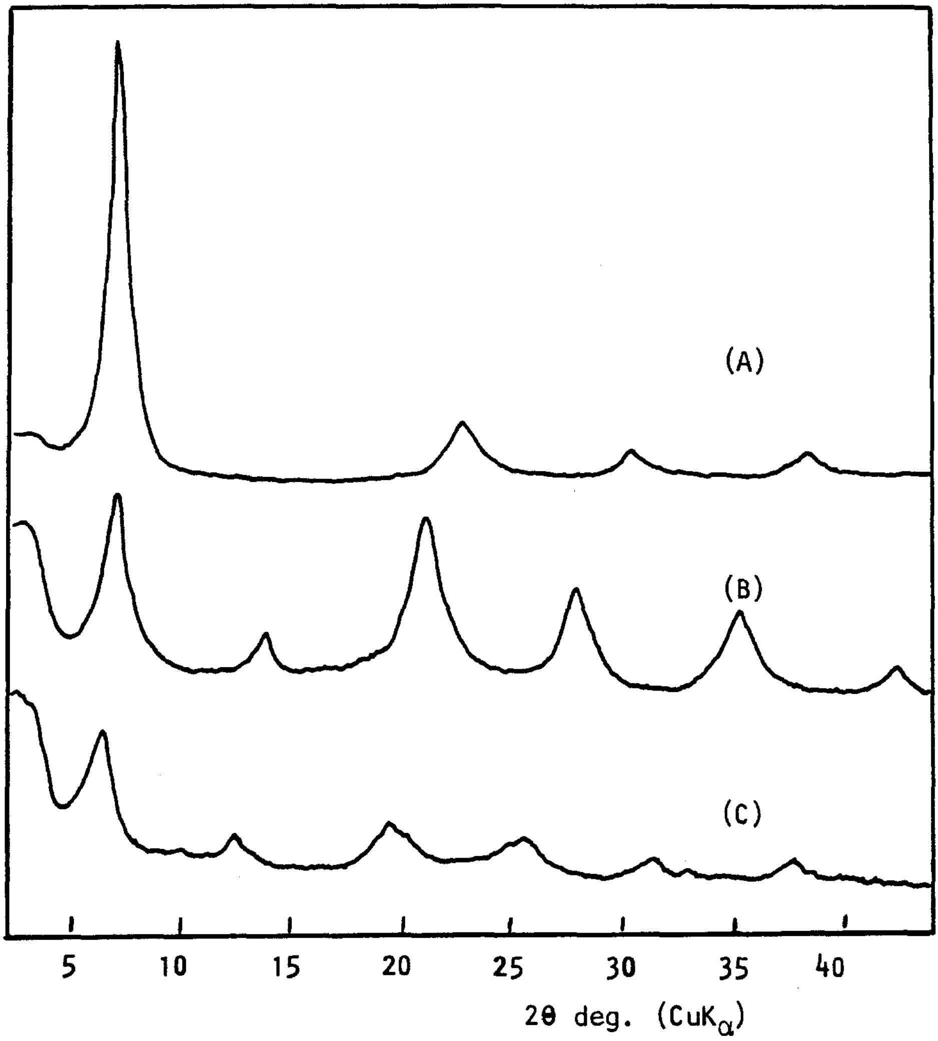

Fig. 2. Cu $K_{\alpha 1}$ X-Ray diffraction patterns of the hydrated vanadium pentoxide matrix (A), and the corresponding intercalation compounds with TPyP (B) and FeTPyP (C).

and δ(VOV) vibrational modes, respectively. The vibrational peaks of the TPyP compound (Figure 3.A) correlates with those of pure TPyP (shown in parentheses): 1632 (1593) ν(CC py), 1600 (1558) ν(CC), 1536 (1540) ν(CC), 1496 (1470) ν(CN), 1424 (1400) ν(CC), 1350 (1350) ν(CN), 1257 (1255) ν(CH), 1088 (1080) δ(CH), 1036 (1001) δ(CH), 1016 (970) δ(NH). A good correlation of the vibrational peaks for the FeTPyP compound (Figure 3.B) is also observed with respect to the pure FeTPyP species (shown in parentheses): 1628 (1625) ν(CC py), 1608 (1605) ν(CC), 1529 (1518) ν(CC), 1504 (1495) ν(CN), 1372 (1350) ν(CN), 1344 (1330)

ν(CN), 1208 (1200) δ(CH), 1032 (1015) δ(CH), 1016 (1000) δ(CH), 842 (840) τ(CH), 802 (790) τ(CH). The tentative assignment was based on the infrared spectra of substituted tetraphenylporphins [36]. In general, the vibrational peaks of the FeTPyP compound are less sensitive to the matrix interactions, indicating a weaker interaction of the porphyrin with the vanadium pentoxide lattice, or with the intercalated water molecules. As a matter of fact the TPyP molecule exhibits two N-pyrrole atoms available for hydrogen bonding, favoring its intercalation in the interlamellar structure.

3.3. CYCLIC VOLTAMMETRY AND SPECTROELECTROCHEMISTRY

The TPyP and FeTPyP intercalation compounds exhibit very broad waves in the range of 0 to 1 V *vs* SHE, in acetonitrile solutions, as shown in Figure 4, ascribed to the $V^{V/IV}$ redox pair in at least two non-equivalent sites in the vanadium oxide matrix. In the case of the FeTPyP compound there is an additional shoulder at 0.4 V, which can be tentatively ascribed to the $Fe^{III/II}$ redox couple. This value is higher than the typical E° of the iron porphyrins in aqueous solution, suggesting that acetonitrile is coordinated to the metal ion.

The electronic spectra of the intercalation compounds, recorded at several applied potentials, are shown in Figure 5. The electronic spectrum of the matrix (not shown in Figure 5) in the oxidized form (e.g. at $E = 0.9$ V) exhibits only a broad band at 380 nm ascribed to a charge-transfer transition within the vanadium(V)-oxide groups. In the reduced form (e.g. at $E = 0$ V) there is a decrease of the charge-transfer band at 380 nm, and an increase of a broad band in the 650–800 nm, ascribed to the ligand field transitions within the V(IV)-oxide chromophore [34]. As one can see in Figure 5, the absorption bands of the vanadium pentoxide matrix appear as base line fluctuations in the spectra of the intercalation compounds; in contrast, the typical absorptions of the porphyrin species are quite evident.

The TPyP compound in the oxidized form (0.9 V) exhibits a strong composite band at 420 nm, involving the vanadium(V)-oxide CT transition and the porphyrin Soret transition. The less intense bands at 650, 595 nm, and at 563, 524 nm are characteristic of the Q_{00} and Q_{10}, or α and β doublets, for the porphyrin free base. When the porphyrin is doubly protonated or metallated, the symmetry is increased and these four bands collapse into two bands, as in the case of the FeTPyP species (Figure 5.B). Therefore, one can conclude that the TPyP species are present as the free base, intercalated into the vanadium pentoxide matrix. The hydrogen bonding with the two N-pyrrole atoms would not allow the four protons to adopt equivalent positions within the porphyrin cavity, in contrast to the doubly protonated porphyrins. The reduction of the matrix (e.g. at $E = -0.10$ V) removes the contribution of the vanadium(V)-oxide CT band around 380 nm, leaving intact the Soret and the Q_{00} and Q_{10} bands and giving rise to the weak, broad, ligand field absorptions above 700 nm.

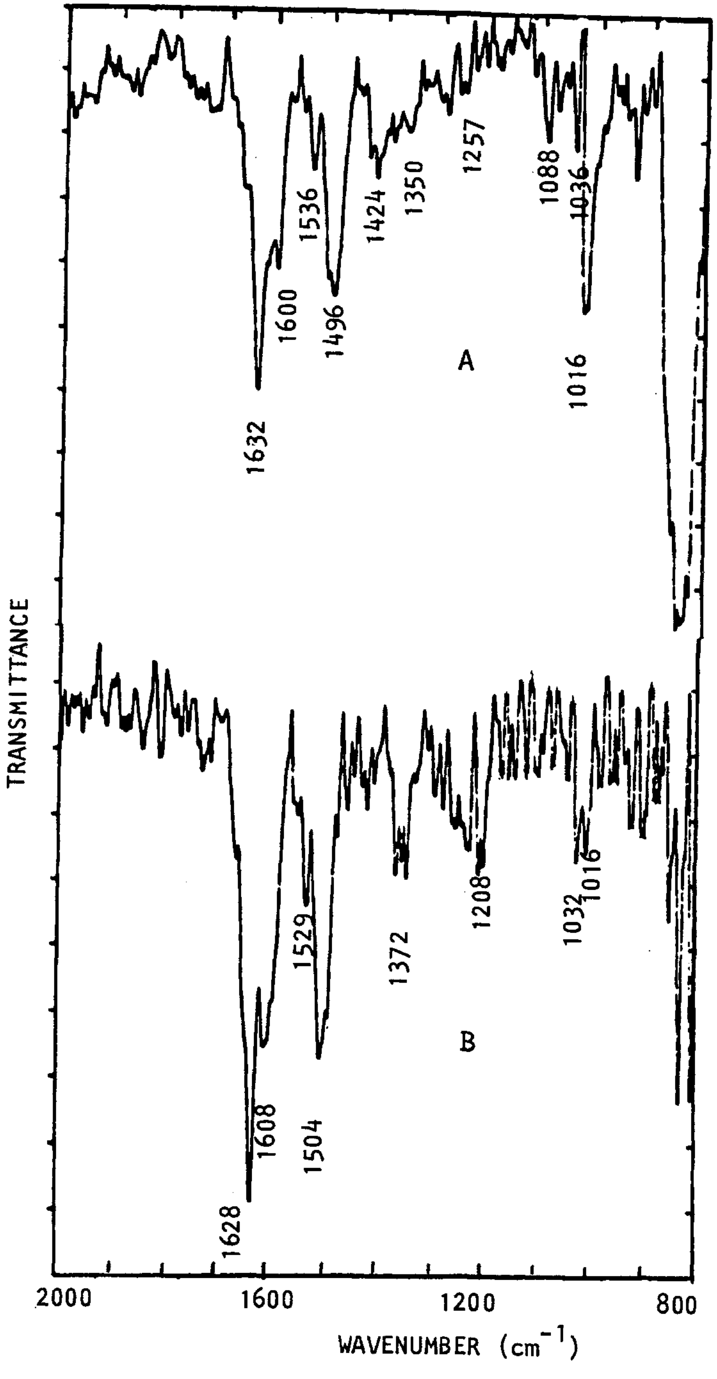

Fig. 3. Reflectance FTIR spectra (1000 scans), of TPyP (A) and FeTPyP (B) intercalated into vanadium pentoxide films.

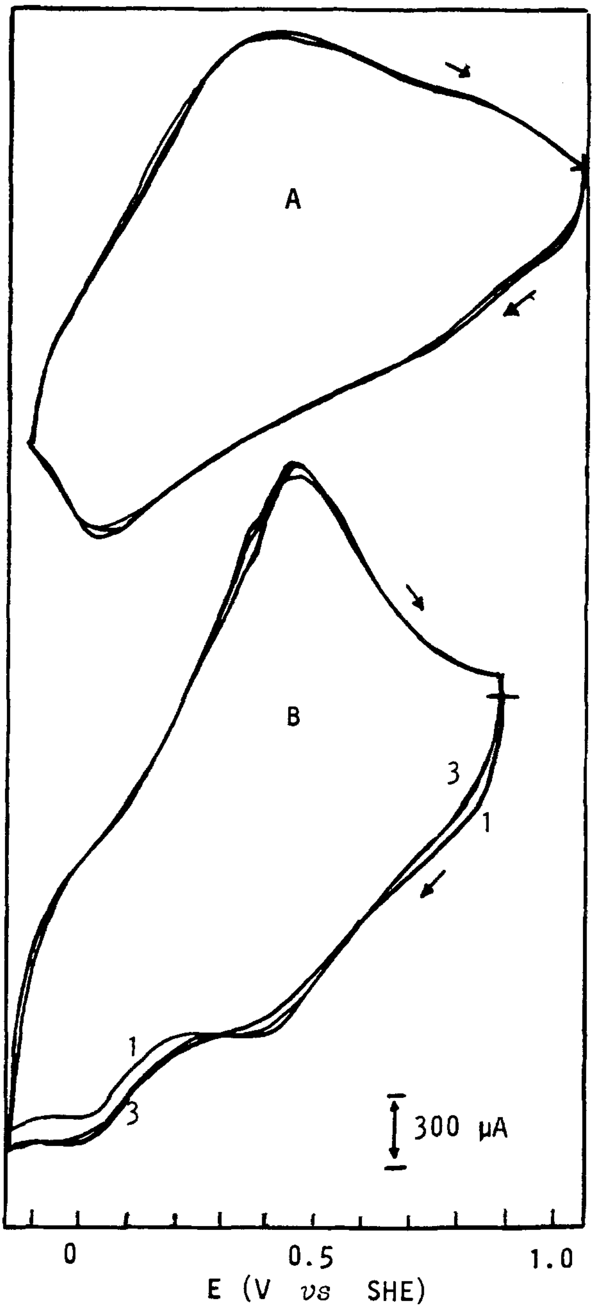

Fig. 4. Cyclic voltammograms of the TPyP (A) and FeTPyP (B) vanadium pentoxide intercalation films on platinum electrodes, at 100 mV s^{-1}, in acetonitrile containing 0.1 M $LiClO_4$.

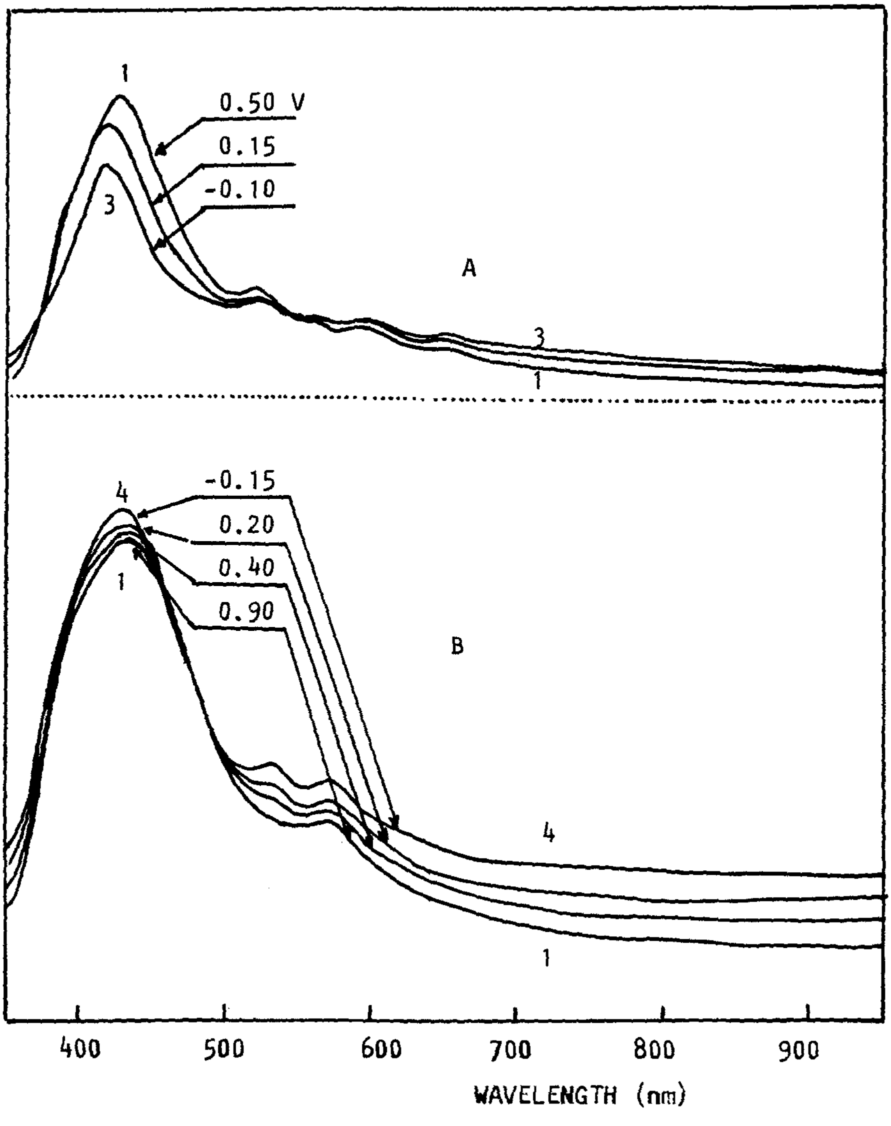

Fig. 5. Electronic spectra of the TPyP (A) and FeTPyP (B) vanadium pentoxide intercalation films on platinum electrodes, at several applied potentials, in acetonitrile containing 0.1 M $LiClO_4$.

The FeTPyP compound in the oxidized form (E = 0.9 V) exhibits a broad band at 440 nm, involving the vanadium(V)-oxide CT transition and the porphyrin Soret transition. In this case, the presence of a Fe(III)-porphyrin is responsible for a bathochromic shift of the Soret band and for the less defined profile for the Q_{00} and Q_{10} bands. When the intercalation compound is in the reduced form (E = −0.15 V) there is an increase in the absorption band at 430 nm, in spite

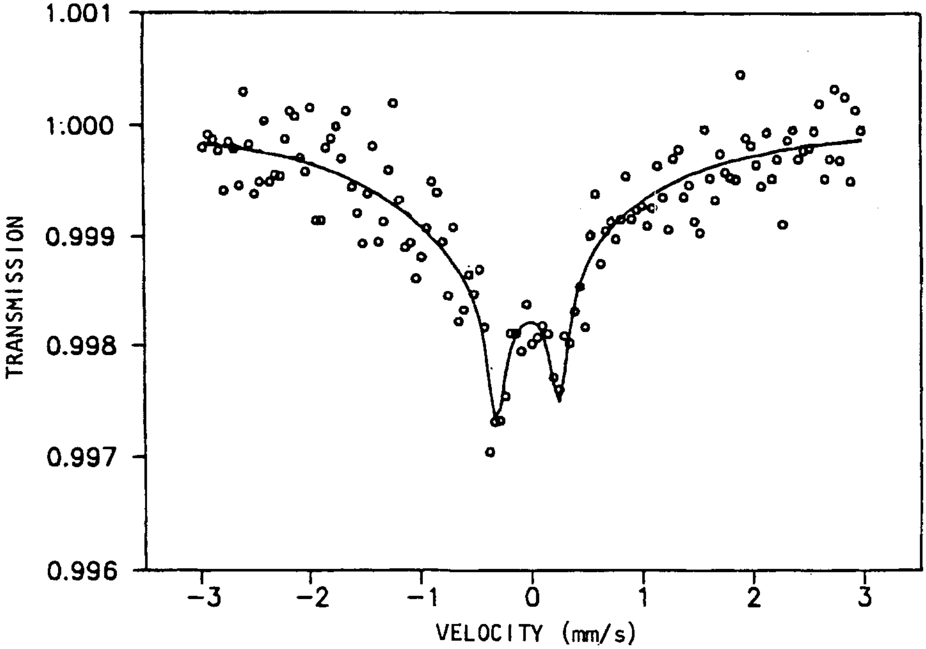

Fig. 6. Mössbauer spectrum of the FeTPyP vanadium pentoxide intercalation compound at room temperature (reference = metallic iron).

of the removal of the contribution of the vanadium(V)-oxide band in this region. The observed increased is due to the fact that the the Soret band is stronger in the case of the Fe(II)-porphyrins. The hypsochromic shift is also consistent with the spectroscopic behavior of the Fe(II)-porphyrins. In the reduced form, the Q_{00} and Q_{10} bands are very well defined, at 572 and 534 nm.

3.4. MÖSSBAUER SPECTRA

The Mössbauer spectrum of the FeTPyP intercalation compound is shown in Figure 6. Despite accumulating data for 2 days the spectrum is still rather noisy, but the main signal can be fitted by a doublet exhibiting a bandwidth of 0.20 ± 0.01 mm s^{-1}, an isomer shift (IS) of 0.10 ± 0.02 mm s^{-1}, and a quadrupole splitting (QS) of 0.56 ± 0.03 mm s^{-1}. This signal is typical of iron complexes in an axial symmetry, such as in the case of the iron porphyrins.

It is known that the FeTPyP species can form dimeric μ-oxo bridged species [37] exhibiting IS = 0.34 mm s^{-1} and QS = 0.60 mm s^{-1}. However, in the case of the FeTPyP intercalation compound, the formation of a dimeric species would lead to a great increase in the interlamellar distance, and this hypothesis can be ruled out.

According to the literature [37], monomeric high-spin iron(III) porphyrins exhibit IS values in the range of 0.2 to 0.5 mm s^{-1}, and QS values in the range of 0.6 to 1.1 mm s^{-1}, while monomeric low-spin iron(III) porphyrins exhibit IS values in the range of 0.10 to 0.25 mm s^{-1} and QS values in the range of 1.25 to 2.30 mm s^{-1}. The monomeric intermediate spin (S = 3/2) iron(III) porphyrins exhibit IS values around 0.3 mm s^{-1} and QS values around 3 mm s^{-1}. The Mössbauer parameters of the FeTPyP intercalation compound do not coincide with any of the monomeric iron(III) porphyrins, but approach the data for the dimeric species. We presume that the FeTPyP are interacting with the V^{V}–O or V^{IV}=O bonds, forming Fe–O–V bridging units, similar to those found in the dimeric $(FeTPyP)_2O$ species. This type of interaction would explain the unusual Mössbauer parameters observed for the FeTPyP intercalation compound.

3.5. ELECTROCATALYTICAL ACTIVITY

The vanadium pentoxide films exhibit only a very weak electrochemical activity, around –0.5 V, in the presence of a saturated dioxygen aqueous solution. In contrast, the FeTPyP intercalation compound exhibits a strong catalytical wave at –0.35 V, as shown in Figure 7, ascribed to the reduction of dioxygen. This wave disappears when dioxygen is replaced by dinitrogen or argon, and is sensitive to the amount of dissolved dioxygen. There is a linear dependence of the catalytic peak currents *versus* the square root of the scan rates, indicating that the process is controlled by the diffusion of the dioxygen molecules to the electrode.

In order to elucidate the nature of the electrochemical process, we carried out an experiment, under identical conditions employed in cyclic voltammetry, using a rotating ring-disc electrode, as shown in Figure 7.B. The platinum ring was kept at +1.4 V, while the potentials of the glassy carbon disc electrode were scanned from +0.2 to –0.7 V. A strong current was observed at the disc electrode at $E_{1/2}$ = –0.35 V, coinciding with the cyclic voltammograms. In contrast, practically no additional current was detected in the ring electrode, indicating that H_2O_2 was not released in the electrocatalytical process. Therefore, according to the rotating ring-disc experiments, the electrochemical reduction of dioxygen proceeds within the vanadium oxide-FeTPyP intercalation compound by a four electron transfer mechanism, forming water.

4. Conclusions

The intercalation of *meso*-tetrapyridylporphyrins into hydrated vanadium(V) pentoxide leads to new electrochemically active materials, exhibiting electrochromic and electrocatalytical properties. The orientation and thickness of TPyP in hydrated vanadium oxide is consistent with a parallel intercalation of the porphyrin, and can be compared with those observed in smectite clays [38].

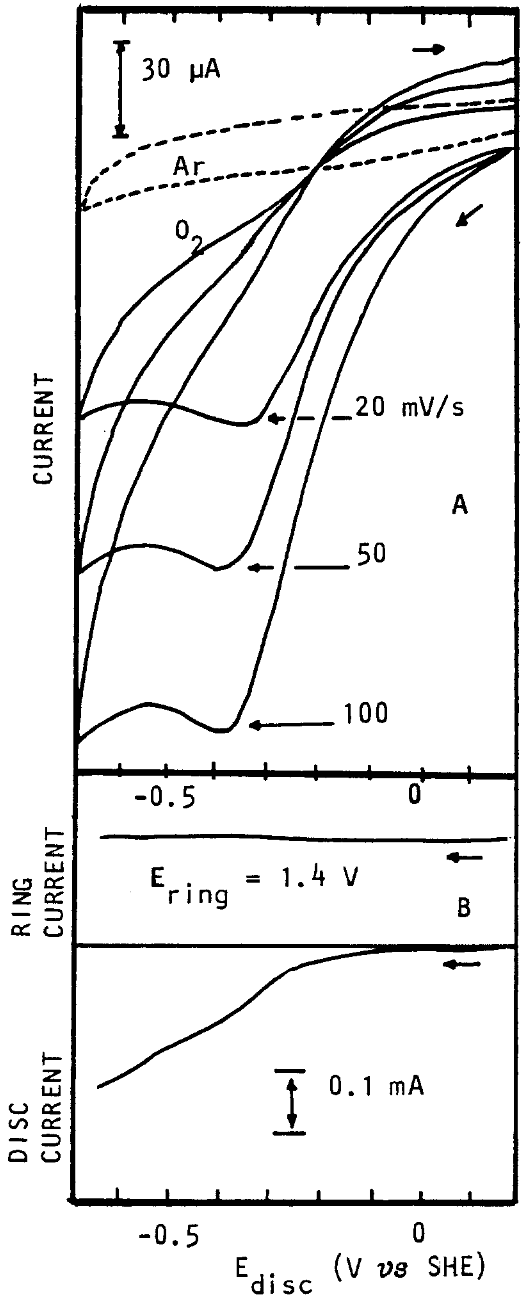

Fig. 7. (A) Cyclic voltammograms of the FeTPyP vanadium pentoxide intercalation film, in aqueous solution containing 1.0 M KCl, phosphate buffer (0.025 M), pH 6.8, under an argon atmosphere (dotted lines) and an oxygen atmosphere at several scan rates, and (B) the corresponding rotating ring-disc voltammograms at 10 mV s^{-1} and 500 rpm.

The high efficiency of the intercalated Fe-TPyP compound in the dioxygen reduction involves a net four electron transfer process and can be ascribed to the confinement of the catalyst within an electron rich environment, represented by the reduced matrix. The confinement is expected to facilitate the complete reduction of dioxygen, since the eventual intermediate species, such as H_2O_2, would be rapidly reduced in the interior of the intercalated compound, before being released from the matrix.

Acknowledgement

We thank Professor Y. Kawano for his help in the XRD and FTIR measurements, K. Araki and F. Matsumoto for their precious assistance in the rotating ring-disc experiments, and Solvay do Brasil (HPO), FAPESP, CNPq and PADCT for financial support.

References

1. J. Livage and R. Collorgues: *Mater. Sci. Eng.* **23**, 297 (1976).
2. J. Bullot, O. Gallais, M. Gauthier, and J. Livage: *App. Phys. Lett.* **36**, 986 (1980).
3. J. Bullot, P. Cordier, O. Gallais, M. Gauthier and J. Livage: *J. Non-Cryst. Solids* **68**, 123 (1984).
4. L. Murawski, C. Gledel, C. Sanchez, J. Livage, and J.P. Audieres: *J. Non-Cryst. Solids* **89**, 98 (1987).
5. K. Bali, L.B. Kiss, T. Szorenyi, M.I. Torok, and I. Hevesi: *J. Phys.* **48**, 431 (1987).
6. G.P. Triberis: *J. Non-Cryst. Solids* **104**, 135 (1988).
7. C.M. Lampert: *Solar Energy Mater.* **11**, 1 (1984).
8. T. Oi: *Ann. Rev. Mater. Sci.* **16**, 185 (1986).
9. A. Donnadieu: *Mater. Sci. Eng.* **B3**, 185 (1989).
10. R.J. Colton, A.M. Guzman, and J.W. Rabalais: *Acc. Chem. Res.* **11**, 170 (1978).
11. Y. Fujita, K. Miyazaki, and C. Tatsuyama: *Jpn. J. Appl. Phys.* **24**, 1082 (1985).
12. T. Yoshino, N. Baba, and Y. Kouda: *Jpn. J. Appl. Phys.* **26**, 782 (1987).
13. J. Livage: *Mat. Res. Bull.* **26**, 1173 (1991).
14. M. Nabani, S. Doeuff, C. Sanches, and J. Livage: *Mat. Sci. Eng.* **B3**, 203 (1989).
15. S.F. Cogan, N.M. Nguyen, S.J. Perrotti, and R.D. Rauh: *J. Appl. Phys.* **66**, 1333 (1989).
16. A.M. Anderson, C.G. Grandqvist, and J.R. Stevens: *Appl. Opt.* **28**, 3295 (1989).
17. P. Aldebert, N. Baffier, N. Gharbi, and J. Livage: *Mat. Res. Bull.* **16**, 669 (1981).
18. J.J. Legendre and J. Livage: *J. Colloid Interfac. Sci.* **94**, 75 (1983).
19. P. Aldebert, N. Baffier, and N. Gharbi: *Mat. Res. Bull.* **16**, 949 (1981).
20. A. Bouhaouss and P. Aldebert: *Mat. Res. Bull.* **18**, 1247 (1983).
21. H. Van Damme, M. Letellier, D. Tinet, B. Kihal, and R. Erre: *Mat. Res. Bull.* **19**, 1635 (1984).
22. H. Masbah, D. Tinet, M. Crespin, R. Erre, R. Setton, and H. Van Damme: *J. Chem. Soc. Chem. Commun.*, 935 (1985).
23. D. Lemordant, A. Bouhaouss, P. Aldebert, and N. Baffier: *J. Chim. Phys.* **83**, 105 (1986).
24. E. Ruiz-Hitzky and B. Casal: *J. Chem. Soc. Faraday Trans. I* **82**, 1597 (1986).
25. T. Nakato, I. Kato, K. Kuroda, and C. Kato: *J. Colloid Interfac. Sci.* **133**, 447 (1989).
26. I. Kato, T. Nakato, K. Kuroda, and C. Kato: *Colloid Surf.* **49**, 241 (1990).
27. R. Erre, H. Masbah, M. Crespin, H. Van Damme: *Solid State Ionics* **37**, 239 (1990).
28. P. Aldebert and V. Paul-Boncour: *Mat. Res. Bull.* **18**, 1263 (1983).
29. T. Nakato, T. Ise, Y. Sugahara, K. Kuroda, and C. Kato: *Mat. Res. Bull.* **26**, 309 (1991).
30. M.G. Kanatzidis, C.G. Wu, H.O. Marcy, and C.R. Kannewurf: *J. Am. Chem. Soc.* **111**, 4139 (1989).

31. C.G. Wu, M.G. Kanatzidis, H.O. Marcy, D.C. DeGroot and C.R. Kannewurf: *Polym. Mat. Sci. Eng.* **61**, 969 (1989).
32. M.G. Kanatzidis, C.G. Wu, H.O. Marcy, D.C. DeGroot, and C.R. Kannewurf: *Chem. Mater.* **2**, 222 (1990).
33. J. Lemerle, L. Nejem, and J. Lefebvre: *J. Inorg. Nucl. Chem.* **42**, 17 (1980).
34. N. Gharbi, C. Sanchez, J. Livage, J. Lemerle, L. Nejem, and J. Lefebvre: *Inorg. Chem.* **21**, 2758 (1982).
35. R. Baddour, J.P. Pereira-Ramos, R. Messina, and J. Perichon: *J. Electroanal. Chem.* **314**, 81 (1991).
36. D.W. Thomas and A.E. Martell: *J. Am. Chem. Soc.* **78**, 1338 (1956).
37. J.R. Sams and T.B. Tsin: in *The Porphyrins*, D. Dolphin Ed., Acad. Press, N.Y. (1979), Vol. IV-B, Ch. 9, p. 425.
38. H. Van Damme, M. Crespin, F. Obrecht, M.I. Cruz, and J.J. Fripiat: *J. Colloid Interfac. Sci.* **66**, 43 (1978).